Int. J. Solids Structures Vol. 30, No. 22, pp. 3159–3170, 1993
Printed in Great Britain

0020–7683/93 $6.00+ .00
© 1993 Pergamon Press Ltd

APPLICATION OF WILSON–RITZ VECTORS IN DYNAMIC SUBSTRUCTURING

M. Lou
Department of Civil Engineering, Dalian University of Technology, Dalian 116023, P.R.C.

and

A. Ghobarah and T. S. Aziz
Department of Civil Engineering and Engineering Mechanics, McMaster University, 1280 Main Street West, Hamilton, Ontario, Canada L8S 4L7

(*Received* 7 *October* 1992; *in revised form* 19 *April* 1993)

Abstract—The basic problems of how to define the spatial load distribution vector when the load-dependent Ritz vectors are applied to the dynamic substructuring using the Component Mode Synthesis (CMS) methods, are identified and discussed. A new definition for spatial load distribution vectors is proposed to avoid the loss of some lower substructural modes if the Wilson–Ritz algorithm is directly used in the modal analysis. The transformation coordinates for the fixed-interface and the free-interface substructures are introduced using the Wilson–Ritz vectors as a substitute of the natural modes of the substructures. Numerical examples validate the new method and demonstrate its accuracy.

1. INTRODUCTION

The development of an efficient numerical technique for the dynamic analysis of large structures with numerous Degrees of Freedom (DOFs) is a valuable task. Component Mode Synthesis (CMS) techniques have been proposed and used in the modal analysis of complex structures (Hurty, 1965; Craig and Bampton, 1968; MacNeal, 1971; Rubin, 1975; Benfield and Hruda, 1971; Wang and Du, 1985). The main computational effort in CMS is to solve the eigenvalue problems for all identified substructures. Reducing this computational effort would be a significant improvement to the CMS techniques.

In recent years, the Wilson–Ritz vectors algorithm (Wilson *et al.*, 1982; Arnold *et al.*, 1985) has been found to be much more efficient than the traditional mode superposition method in analysing forced vibration structures. Encouraged by its efficiency, several researchers (Wilson and Bay, 1986; Abdallah and Huckelbridge, 1990; Lou and Lian, 1989), attempted to introduce the Wilson–Ritz vectors algorithm into the CMS techniques for dynamic substructuring. The static Ritz vectors are load-dependent. The first Ritz vector may be directly obtained from the spatial load distribution vector of the dynamic loading acting on the structure. Then, other Ritz vectors are recurrently produced from the previous ones. Some Ritz vectors, which are orthogonal with respect to the spatial load distribution vector, will not appear in the set of the obtained Ritz vectors. This is considered to be one of the advantages of the Wilson–Ritz algorithm when it is used in analyzing specific forced vibration structural problems. In an extreme special case, for example, the asymmetric Ritz vectors are not generated at all if a perfectly symmetric structure, which is subjected to a perfectly symmetric dynamic loading, is analysed. These asymmetric Ritz vectors would not contribute to the dynamic response of the structure. Therefore, their inclusion is not required. On the other hand, when the Wilson–Ritz algorithm is applied to the modal analysis of the substructures, this feature would not be advantageous any more. In fact, such a feature is problematic. In this case, it is essential to include all the lower modes of the substructures in CMS techniques. The possibility of losing some of the lower modes of the substructures, when the Wilson–Ritz algorithm is applied to the modal analysis of substructures in CMS methods, constitutes a fundamental problem that needs to be solved. Another problem would arise for free vibration of structures since there is no spatial load distribution vector present. Therefore, another fundamental problem is how to establish the spatial load distribution vector for every substructure when the Wilson–Ritz algorithm is applied to CMS methods. A correct definition for this spatial load distribution vector should ensure that the continuous lower modes of every substructure can be composed using the Ritz vectors obtained recurrently from this spatial load distribution vector.

The objective of this study is to present a new definition for the spatial load distribution vector and to establish the necessary formulation of the fixed-interface and the free-interface CMS methods using the Wilson–Ritz algorithm for dynamic substructuring.

2. REDUCED STIFFNESS MATRIX IN THE RITZ VECTORS SUBSPACE

Load-dependent Ritz vectors can be generated recurrently using the Wilson–Ritz algorithm in terms of the stiffness matrix [K] and mass matrix [M] of the structure as well as the spatial load distribution vector {f(s)} of the dynamic loading applied to the structure. The generation process involves the following steps:

(1) Solve for the primary static vectors $\{\mathbf{X}_j^*\}$, $j = 1, \ldots, m$

$$[\mathbf{K}]\{\mathbf{X}_j^*\} = \{\mathbf{f}_j\}, \tag{1}$$

where

$$\{\mathbf{f}_j\} = \begin{Bmatrix} \{\mathbf{f(s)}\} & (j = 1) \\ [\mathbf{M}]\{\mathbf{X}_{j-1}\} & (j > 1) \end{Bmatrix}. \tag{2}$$

(2) Orthogonalize with respect to [M] and the previous Ritz vectors

$$\{\mathbf{X}_j^{**}\} = \{\mathbf{X}_j^*\} - \sum_{k=1}^{j-1} c_{jk}\{\mathbf{X}_k\}, \tag{3}$$

where

$$c_{jk} = \begin{Bmatrix} 0 & j = 1 \\ \{\mathbf{X}_j^*\}^{\mathrm{T}}[\mathbf{M}]\{\mathbf{X}_k\} & j > 1 \end{Bmatrix}. \tag{4}$$

(3) Normalize with respect to [M] in order to determine the final Ritz vector $\{\mathbf{X}_j\}$, thus

$$\{\mathbf{X}_j\} = \alpha_j\{\mathbf{X}_j^{**}\}, \tag{5}$$

where

$$\alpha_j = [\{\mathbf{X}_j^{**}\}^{\mathrm{T}}[\mathbf{M}]\{\mathbf{X}_j^{**}\}]^{-1/2}. \tag{6}$$

These m obtained Ritz vectors [X] span a new subspace for the solution of the eigenproblem of the structure. In general, the reduced stiffness matrix of the structure in the subspace can be written as

$$[\mathbf{K}^*] = [\mathbf{X}]^{\mathrm{T}}[\mathbf{K}][\mathbf{X}]. \tag{7}$$

[K*] may be determined in practice by using a recurrence relationship instead of eqn (7) as follows:

$$\begin{aligned} \{\mathbf{P}_1\} &= [\mathbf{K}]\{\mathbf{X}_1\} \\ &= \alpha_1\{\mathbf{f(s)}\} \end{aligned} \tag{8a}$$

and for $j > 1$

$$\{\mathbf{P}_j\} = [\mathbf{K}]\{\mathbf{X}_j\}$$
$$= \alpha_j[\mathbf{K}]\left[\{\mathbf{X}_j^*\} - \sum_{k=1}^{j-1} c_{jk}\{\mathbf{X}_k\}\right]$$
$$= \alpha_j\left[\{\mathbf{f}_j\} - \sum_{k=1}^{j-1} c_{jk}\{\mathbf{P}_k\}\right]. \tag{8b}$$

The recurrence formula defining the elements of the jth row in $[\mathbf{K}^*]$ can be deduced from eqns (8a) and (8b). The first element k_{j1}^* in the jth row in $[\mathbf{K}^*]$ can be expressed by the following equation:

$$k_{j1}^* = \{\mathbf{X}_j\}^{\mathrm{T}}[\mathbf{K}]\{\mathbf{X}_1\}$$
$$= \alpha_1\{\mathbf{X}_j\}^{\mathrm{T}}\{\mathbf{f(s)}\}. \tag{9a}$$

Other elements, k_{jk}^*, where $k \leqslant j$, can be written as follows:

$$k_{jk}^* = \{\mathbf{X}_j\}^{\mathrm{T}}\{\mathbf{P}_k\}$$
$$= \alpha_k\left[\{\mathbf{X}_j\}^{\mathrm{T}}\{\mathbf{f}_k\} - \sum_{l=1}^{k-1} c_{kl}\{\mathbf{X}_j\}^{\mathrm{T}}\{\mathbf{P}_l\}\right]$$
$$= -\alpha_k \sum_{l=1}^{k-1} c_{kl} k_{jl}^* \quad (k \leqslant j), \tag{9b}$$

where it is implied that $\{\mathbf{X}_j\}^{\mathrm{T}}\{\mathbf{f}_k\}$ is equal to zero due to the orthogonality of the Ritz vectors since $\{\mathbf{f}_k\}$ is equal to $[\mathbf{M}]\{\mathbf{X}_{k-1}\}$ as given by eqn (2).

Thus, due to its symmetry, the whole reduced stiffness matrix of the structure can be determined such that

$$k_{kj}^* = k_{jk}^* \quad (k > j). \tag{9c}$$

In eqn (9b), all previous $(k-1)$ elements, k_{jk}^*, in the jth row of $[\mathbf{K}^*]$ are already generated. Equation (9b) indicates that the reduced stiffness matrix in the subspace spanned by Ritz vectors can be recurrently determined in terms of the obtained Ritz vectors $\{\mathbf{X}_j\}$, the spatial load distribution vector $\{\mathbf{f(s)}\}$, and the normalizing and orthogonalizing factors α_j and c_{jk}, respectively. The relationship defined in eqns (9a) and (9b) can be used in place of the transformation as defined in eqn (7).

3. SPATIAL DISTRIBUTION VECTOR FOR SUBSTRUCTURES

Once the spatial load distribution vector is defined, the Ritz vectors can be generated for a given substructure based on the previous formulation. Four methods are available in order to define the spatial distribution vector for a given substructure as follows:

(a) The first method defines the substructure spatial load distribution vector as the subvector of the spatial distribution vector of the actual external load for the total structure. This was used by Wilson *et al.* (1986) in the fixed-interface CMS method;

(b) The second method uses the inertial force vector generated by a uniform unit acceleration applied to the substructure. This was used by Lou and Lian (1989) in the free-interface CMS method. Thus, for the ith substructure, the spatial distribution vector is given by:

$$\{\mathbf{f}_i(\mathbf{s})\} = [\mathbf{M}_i]\{\mathbf{I}_i\}, \tag{10}$$

where $[\mathbf{M}_i]$ is the mass matrix of the ith substructure and all elements in $\{\mathbf{I}_i\}$ are equal to unity;

(c) The third method is the inertial force vector generated by the static constraint modes of the fixed-interface substructure. This was used by Abdallah and Huckelbridge (1990) in the fixed-interface CMS methods. Thus,

$$\{\mathbf{f}_i^j(\mathbf{s})\} = [\mathbf{M}_i^{\mathrm{II}}]\{\psi_{c,i}^j\} \quad (j = 1, 2, \ldots, N_i^{\mathrm{B}}), \tag{11}$$

where $\{\psi_{c,i}^j\}$ is the jth column in the constraint mode matrix $[\boldsymbol{\Psi}_{c,i}]$ of the ith substructure, $[\mathbf{M}_i^{\mathrm{II}}]$ is the partial mass matrix of the substructure considering the internal DOFs only, and N_i^{B} is the number of the boundary DOFs on the fixed-interface of the ith substructure;

(d) The fourth method is the inertial force vector generated by the static attachment modes of the free-interface substructure, and it was used by Abdallah and Huckelbridge (1990) in the free-interface CMS method:

$$\{\mathbf{f}_i^j(\mathbf{s})\} = [\mathbf{M}_i]\{\psi_{a,i}^j\} \quad (j = 1, 2, \ldots, N_i^{\mathrm{B}}), \tag{12}$$

where $\{\psi_{a,i}^j\}$ is the jth column in the attachment mode matrix $[\boldsymbol{\Psi}_{a,i}]$ of the ith substructure, $[\mathbf{M}_i]$ is the total mass matrix of the substructure, and N_i^{B} is the number of boundary DOFs on the free-interface of the ith substructure.

The lower continuous modes of a substructure may not be obtained when the first and second definitions of the spatial load distribution vector are employed. As an example, the case of a symmetric substructure subjected to a symmetric and an asymmetric inertial force may be encountered. In such a case, losing half of the required Ritz vectors is inevitable. This problem would be solved when either the third or the fourth definitions of the spatial distribution vector is employed. However, a different problem will arise for these definitions as follows:

Consider N_i^{I} to be the order of $[\mathbf{M}_i^{\mathrm{II}}]$ or $[\mathbf{M}_i]$. Thus, the total number of Ritz vectors that can be obtained from eqn (11) or eqn (12) is $(N_i^{\mathrm{B}} \times N_i^{\mathrm{I}})$ since N_i^{I} Ritz vectors can be generated from each constraint mode $\{\psi_{c,i}^j\}$ or attachment mode $\{\psi_{a,i}^j\}$. Out of these $(N_i^{\mathrm{B}} \times N_i^{\mathrm{I}})$ Ritz vectors, only N_i^{I} are basic independent vectors and the rest are dependent upon these basic ones. Following the Wilson–Ritz algorithm, the relationship between the obtained Ritz vectors, when they are less than N_i^{I}, can be achieved using the concept of orthogonalization with respect to the mass matrix. However, when N_i^{B} is greater than the number of the required Ritz vectors, $\mathbf{m}$, it would be difficult to determine which $\{\psi_{c,i}^j\}$ would be used in generating the Ritz vectors using eqn (11), or $\{\psi_{a,i}^j\}$ using eqn (12). In this case, some $\{\psi_{c,i}^j\}$ or $\{\psi_{a,i}^j\}$ will not be used.

Therefore, it is necessary to find a definition for the spatial distribution vector $\{\mathbf{f}_i(\mathbf{s})\}$ in order to apply the Wilson–Ritz algorithm to the modal analysis of substructures in CMS methods. The form of the vector $\{\mathbf{f}_i(\mathbf{s})\}$ is proposed as an inertial force, similar to the definitions in eqns (10), (11) and (12) and is given by:

$$\{\mathbf{f}_i(\mathbf{s})\} = [\mathbf{M}_i]\{\mathbf{w}_i\}, \tag{13}$$

where $[\mathbf{M}_i]$ will be replaced by $[\mathbf{M}_i^{\mathrm{II}}]$ in the case of the fixed-interface CMS method. $\{\mathbf{w}_i\}$ is a general weighting function vector. Two factors are considered in establishing $\{\mathbf{w}_i\}$. First, $\{\mathbf{w}_i\}$ has to be as close as possible to the first mode shape vector, based on the premise that the first mode shape of each substructure must be included in the synthesis procedure of the system. Hence, an improved form for eqn (10) can be adopted for the inertia vector in this first step as

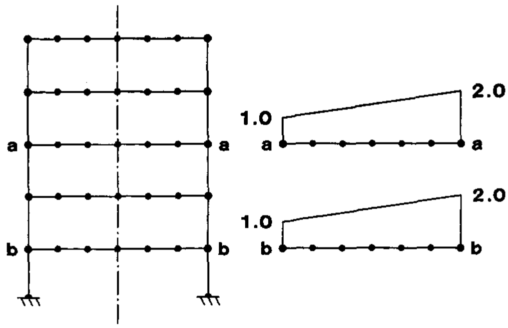

Fig. 1. Frame structure and its symmetrical function.

$$\{l_i\} = [\mathbf{K}_i]^{-1}[\mathbf{M}_i]\{\mathbf{I}_i\}. \tag{14}$$

This improvement is based upon an improved Rayleigh method. Subsequently, it is necessary to take the symmetry of the substructure into account, as mentioned above. A symmetry function vector, $\{\mathbf{S}_i\}$, is introduced for the case of symmetrical substructures. In general, the inertial force acting on a symmetrical substructure can be decomposed into symmetrical and asymmetrical components. A trapezoidal distribution is taken along the nodes on the same symmetrical planes or lines. As an example, for the case of the symmetrical frame shown in Fig. 1, the inertial forces are assumed to have a trapezoidal distribution for each level of the frame. Finally, the weighting function $\{\mathbf{w}_i\}$ is composed of $\{l_i\}$ and $\{\mathbf{S}_i\}$, i.e. the jth element of $\{\mathbf{w}_i\}$ is equal to the product of the jth elements of both $\{l_i\}$ and $\{\mathbf{S}_i\}$,

$$w_{i,j} = l_{i,j} \cdot S_{i,j}. \tag{15}$$

This new spatial distribution vector accounts for the effect of the first mode shape as well as the effect of the symmetry of the substructure. Each element in $\{\mathbf{S}_i\}$ would be equal to unity in case the substructure is not symmetrical.

4. COORDINATE TRANSFORMATION FOR FIXED-INTERFACE SUBSTRUCTURE

The stiffness and mass matrices of the ith substructure are divided into submatrices according to the internal and interface DOFs as follows:

$$[\mathbf{K}_i] = \begin{bmatrix} \mathbf{K}_i^{\mathrm{II}} & \mathbf{K}_i^{\mathrm{IB}} \\ \mathbf{K}_i^{\mathrm{BI}} & \mathbf{K}_i^{\mathrm{BB}} \end{bmatrix} \tag{16}$$

and

$$[\mathbf{M}_i] = \begin{bmatrix} \mathbf{M}_i^{\mathrm{II}} & 0 \\ 0 & \mathbf{M}_i^{\mathrm{BB}} \end{bmatrix}, \tag{17}$$

where the superscripts I and B represent the internal and boundary interface DOFs.

The Ritz vectors $[\mathbf{X}_i]$ of the ith substructure can be recurrently generated from $[\mathbf{K}_i^{\mathrm{II}}]$, $[\mathbf{M}_i^{\mathrm{II}}]$ and $\{\mathbf{f}_i(\mathbf{s})\}$ using the Wilson–Ritz algorithm. The constraint modes $[\mathbf{\Psi}_{c,i}]$ can be obtained using the relation

$$[\mathbf{\Psi}_{c,i}] = -[\mathbf{K}_i^{\mathrm{II}}]^{-1}[\mathbf{K}_i^{\mathrm{IB}}]. \tag{18}$$

Thus, the coordinate transformation for the ith substructure may be written as

$$\begin{Bmatrix} u_i^{\mathrm{I}} \\ u_i^{\mathrm{B}} \end{Bmatrix} = \begin{bmatrix} \mathbf{X}_i & \mathbf{\Psi}_{c,i} \\ 0 & \mathbf{I}_i \end{bmatrix} \begin{Bmatrix} q_i \\ u_i^{\mathrm{B}} \end{Bmatrix} = [\mathbf{T}_i] \begin{Bmatrix} q_i \\ u_i^{\mathrm{B}} \end{Bmatrix}. \tag{19}$$

The generalized stiffness and mass matrices after finishing the coordinate transformation are given as

$$[\bar{\mathbf{K}}_i] = [\mathbf{T}_i]^{\mathrm{T}}[\mathbf{K}_i][\mathbf{T}_i] = \begin{bmatrix} \mathbf{K}_i^* & 0 \\ 0 & \mathbf{K}_i^{\mathrm{BB}} + \mathbf{K}_i^{\mathrm{BI}}\mathbf{\Psi}_{c,i} \end{bmatrix} \tag{20}$$

and

$$[\bar{\mathbf{M}}_i] = [\mathbf{T}_i]^{\mathrm{T}}[\mathbf{M}_i][\mathbf{T}_i] = \begin{bmatrix} \mathbf{I} & \mathbf{X}_i^{\mathrm{T}}\mathbf{M}_i^{\mathrm{II}}\mathbf{\Psi}_{c,i} \\ \mathbf{\Psi}_{c,i}^{\mathrm{T}}\mathbf{M}_i^{\mathrm{II}}\mathbf{X}_i & \mathbf{M}_i^{\mathrm{BB}} + \mathbf{\Psi}_{c,i}^{\mathrm{T}}\mathbf{M}_i^{\mathrm{II}}\mathbf{\Psi}_{c,i} \end{bmatrix}, \tag{21}$$

where $[\mathbf{K}_i^*] = [\mathbf{X}_i]^{\mathrm{T}}[\mathbf{K}_i][\mathbf{X}_i]$ can be determined by eqns (9a) and (9b).

Once the generalized stiffness and mass matrices of all substructures are generated, the generalized stiffness and mass matrices of the whole system can be assembled similar to the assembling of the stiffness matrix of a structure using the finite element method. Therefore,

$$[\bar{\mathbf{K}}] = \sum_{i=1}^{n} [\boldsymbol{\alpha}_i]^{\mathrm{T}}[\bar{\mathbf{K}}_i][\boldsymbol{\alpha}_i] \tag{22}$$

and

$$[\bar{\mathbf{M}}] = \sum_{i=1}^{n} [\boldsymbol{\alpha}_i]^{\mathrm{T}}[\bar{\mathbf{M}}_i][\boldsymbol{\alpha}_i], \tag{23}$$

where n is the number of substructures.

5. COORDINATE TRANSFORMATION FOR FREE-INTERFACE SUBSTRUCTURES

In this section, only the case of free-interface substructure that has no rigid-body modes is considered. The case of the substructure that has rigid-body modes has been discussed previously in the work by Abdallah and Huckelbridge (1990). Once the Ritz vectors are obtained, the first step, for establishing the coordinate transformation for the free-interface substructure, is to determine the residual flexibility matrix, $[\mathbf{F}_{c,i}]$. It can be written in the form

$$[\mathbf{F}_{c,i}] = [\mathbf{K}_i]^{-1} - [\mathbf{X}_i]([\mathbf{X}_i]^{\mathrm{T}}[\mathbf{K}_i][\mathbf{X}_i])^{-1}[\mathbf{X}_i]^{\mathrm{T}} = [\mathbf{K}_i]^{-1}([\mathbf{I}] - [\mathbf{K}_i][\mathbf{X}_i][\mathbf{K}_i^*]^{-1}[\mathbf{X}_i]^{\mathrm{T}}).$$

Substituting eqn (8), then

$$[\mathbf{F}_{c,i}] = [\mathbf{K}_i]^{-1}([\mathbf{I}] - [\mathbf{P}_i][\mathbf{K}_i^*]^{-1}[\mathbf{X}_i]^{\mathrm{T}}). \tag{24}$$

The computational effort for the inversion of $[\mathbf{K}_i^*]$, with a small size, will be much less than the computational effort for the orthogonalization and normalization of the Ritz vectors $[\mathbf{X}_i]$. When $[\mathbf{M}_i]$ is a lumped mass matrix, the orthogonalization of the Ritz vectors is performed with respect to the stiffness matrix rather than the mass matrix $[\mathbf{M}_i]$, as $[\mathbf{K}_i^*]$ can be easily obtained using eqns (9a) and (9b). The residual flexibility matrix can also be defined as (Lou and Lian, 1989):

$$[\mathbf{F}_{c,i}] = [\mathbf{K}_i]^{-1}([\mathbf{I}] - [\mathbf{M}_i][\mathbf{X}_i][\mathbf{X}_i]^{\mathrm{T}}). \tag{25}$$

Regardless of using eqn (24) or eqn (25), $[\mathbf{F}_{c,i}]$ may be written in the form

$$[\mathbf{F}_{c,i}] = [\mathbf{K}_i]^{-1}[\mathbf{G}_i^{\mathrm{I}}, \mathbf{G}_i^{\mathrm{B}}]. \tag{26}$$

Therefore, the residual attachment modes $[\boldsymbol{\Psi}_{a,i}]$ of the free-interface substructure can be defined as

$$[\boldsymbol{\Psi}_{a,i}] = [\mathbf{K}_i]^{-1}[\mathbf{G}_i^{\mathrm{B}}]. \tag{27}$$

Taking advantage of the triangular decomposition of $[\mathbf{K}_i]$, defined by eqn (1), in determining the Ritz vectors $[\mathbf{X}_i]$, $[\boldsymbol{\Psi}_{a,i}]$, defined by eqn (27), can be easily obtained by solving linear algebraic equations (N_i^{B} times) rather than solving for the inversion of $[\mathbf{K}_i]$.

The first coordinate transformation matrix $[\mathbf{T}_{i1}]$ is composed of the Ritz vectors $[\mathbf{X}_i]$ and the residual attachment modes $[\boldsymbol{\Psi}_{a,i}]$. It expresses the relationship between the physical coordinates and the model coordinates as well as the interface force as follows:

$$\begin{aligned} \{\mathbf{u}_i\} &= [\mathbf{X}_i, \boldsymbol{\Psi}_{a,i}]\begin{Bmatrix} q_i \\ f_{a,i} \end{Bmatrix} \\ &= [\mathbf{T}_{i1}]\begin{Bmatrix} q_i \\ f_{a,i} \end{Bmatrix}. \end{aligned} \tag{28}$$

The generalized stiffness and mass matrices of the free-interface substructure, after the first coordinate transformation is determined, are

$$\begin{aligned} [\hat{\mathbf{K}}_i] &= [\mathbf{T}_{i1}]^{\mathrm{T}}[\mathbf{K}_i][\mathbf{T}_{i1}] \\ &= \begin{bmatrix} \mathbf{X}_i^{\mathrm{T}}\mathbf{K}_i\mathbf{X}_i & \mathbf{X}_i^{\mathrm{T}}\mathbf{K}_i\boldsymbol{\Psi}_{a,i} \\ \boldsymbol{\Psi}_{a,i}^{\mathrm{T}}\mathbf{K}_i\mathbf{X}_i & \boldsymbol{\Psi}_{a,i}^{\mathrm{T}}\mathbf{K}_i\boldsymbol{\Psi}_{a,i} \end{bmatrix} \\ &= \begin{bmatrix} \mathbf{K}_i^* & \mathbf{X}_i^{\mathrm{T}}\mathbf{G}_i^{\mathrm{B}} \\ [\mathbf{G}_i^{\mathrm{B}}]^{\mathrm{T}}\mathbf{X}_i & \boldsymbol{\Psi}_{a,i}^{\mathrm{T}}\mathbf{G}_i^{\mathrm{B}} \end{bmatrix} \end{aligned} \tag{29}$$

and

$$\begin{aligned} [\hat{\mathbf{M}}_i] &= [\mathbf{T}_{i1}]^{\mathrm{T}}[\mathbf{M}_i][\mathbf{T}_{i1}] \\ &= \begin{bmatrix} \mathbf{I} & \mathbf{X}_i^{\mathrm{T}}\mathbf{M}_i\boldsymbol{\Psi}_{a,i} \\ \boldsymbol{\Psi}_{a,i}^{\mathrm{T}}\mathbf{M}_i\mathbf{X}_i & \boldsymbol{\Psi}_{a,i}^{\mathrm{T}}\mathbf{M}_i\boldsymbol{\Psi}_{a,i} \end{bmatrix}. \end{aligned} \tag{30}$$

Analogous to the conventional method of the free-interface CMS, the second coordinate transformation matrix $[\mathbf{T}_{i2}]$ can be formed, taking advantage of the double compatability conditions at the interface. It expresses the relationship between the local coordinates in substructure and the global modal coordinates such that

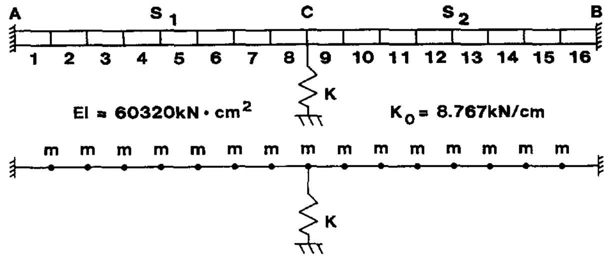

Fig. 2. A uniform beam and its substructure division.

$$\begin{Bmatrix} q_i \\ f_{a,i} \end{Bmatrix} = [\mathbf{T}_{i2}]\{\mathbf{q}\}. \tag{31}$$

The final reduced stiffness and mass matrices of the whole system can be obtained by assembling the reduced stiffness and mass matrices of the substructure, thus

$$[\bar{\mathbf{K}}] = \sum_{i=1}^{n} [\mathbf{T}_{i2}]^{\mathrm{T}}[\hat{\mathbf{K}}_i][\mathbf{T}_{i2}] \tag{32}$$

and

$$[\bar{\mathbf{M}}] = \sum_{i=1}^{n} [\mathbf{T}_{i2}]^{\mathrm{T}}[\hat{\mathbf{M}}_i][\mathbf{T}_{i2}]. \tag{33}$$

6. NUMERICAL EXAMPLES

Two examples are analysed in order to demonstrate the new definition suggested for the spatial distribution vector.

(1) *Example 1*

A uniform beam, fixed at both ends and supported on a spring at mid-span, was analysed previously by Abdallah and Huckelbridge (1990). The same beam is considered here. The beam is discretized into 16 elements as shown in Fig. 2 such that each node has two degrees of freedom. The mass of each element is lumped at its two ends. The full beam structure is divided into two substructures at section C. The first substructure includes elements 1–8, while the second substructure includes elements 9–16. Both techniques of mode synthesis and Ritz vector synthesis are applied to the free-interface substructure and the fixed-interface substructure methods in order to determine the first five modes of the beam.

(i) *Results from the fixed-interface substructure method.* Fixing section C results in two symmetrical substructures. Accordingly, symmetrical functions are considered in determining the weighted function vector, defined in eqns (13) and (15). Three computational cases are performed for comparison purposes:

(a) Case 1—$R(3)$, in which three Ritz vectors for each substructure in addition to two constraint modes are employed in the analysis, thus, a total of eight generalized degrees of freedom are assigned to the full beam;

(b) Case 2—$M(2)$, in which two natural modes for each substructure in addition to two constraint modes, are employed in the analysis, thus, a total of six generalized degrees of freedom are assigned to the full beam; and,

(c) Case 3—$M(3)$, in which three natural modes for each substructure in addition to two constraint modes are employed in the analysis, thus, a total of eight generalized degrees of freedom are assigned to the full beam.

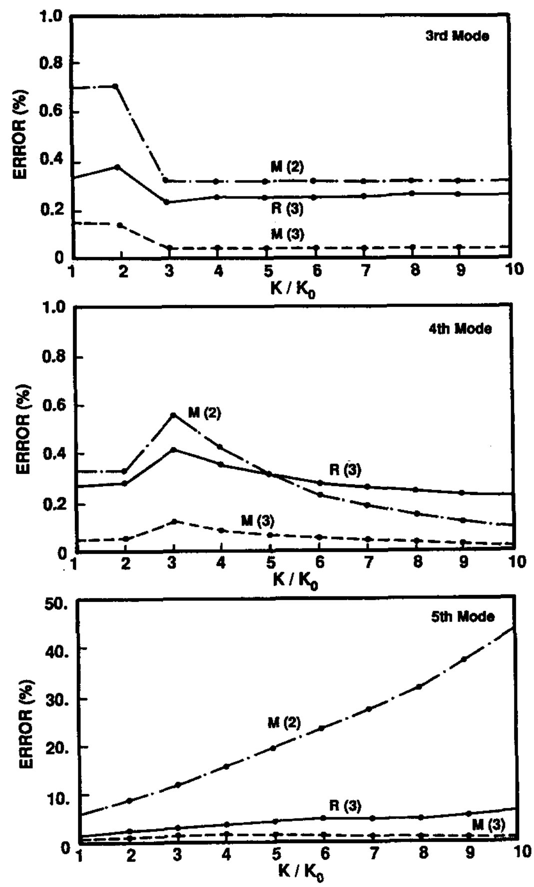

Fig. 3. The relative errors in the natural frequencies of the uniform beam (using fixed-substructure method).

The relative errors in estimating the natural frequencies of the full beam, when compared to the values of the natural frequencies obtained directly using the finite element method are determined for all the three cases and over a range of the middle spring stiffness. The relative errors associated with the first two natural frequencies are found to be nearly equal to zero for all three cases. For the third, fourth and fifth natural frequencies, the relative error behavior results are shown in Fig. 3. The figure shows that errors for the third and fourth natural frequencies are small and within the practical acceptable limits. As expected, the error in the fifth natural frequency is large for the case of considering only two natural modes for each substructure. There appears to be a tendency for the fourth mode frequency error to peak around a value K/K_0 equal to 3. However, similar behavior cannot be observed for the third or the fifth mode frequencies.

(ii) *Results from the free-interface substructure method.* For both free-interface substructures, the two degrees of freedom at section C are assumed free. No symmetry feature for the resulting cantilever beams exists. Thus, the symmetry function vector, $\{\mathbf{S}_i\}$, is set equal to a unity vector when eqn (13) is employed in forming the spatial distribution vector, $\{\mathbf{f}_i(\mathbf{s})\}$. The stiffness of the supporting spring would be introduced when the second coordinate transformation matrix, $[\mathbf{T}_{i2}]$, is formed. Four computational cases are performed. These are:

(a) Case 1—$R(4)$, in which four Ritz vectors for each substructure are employed in the analysis;

(b) Case 2—$R(5)$, in which five Ritz vectors for each substructure are employed in the analysis;

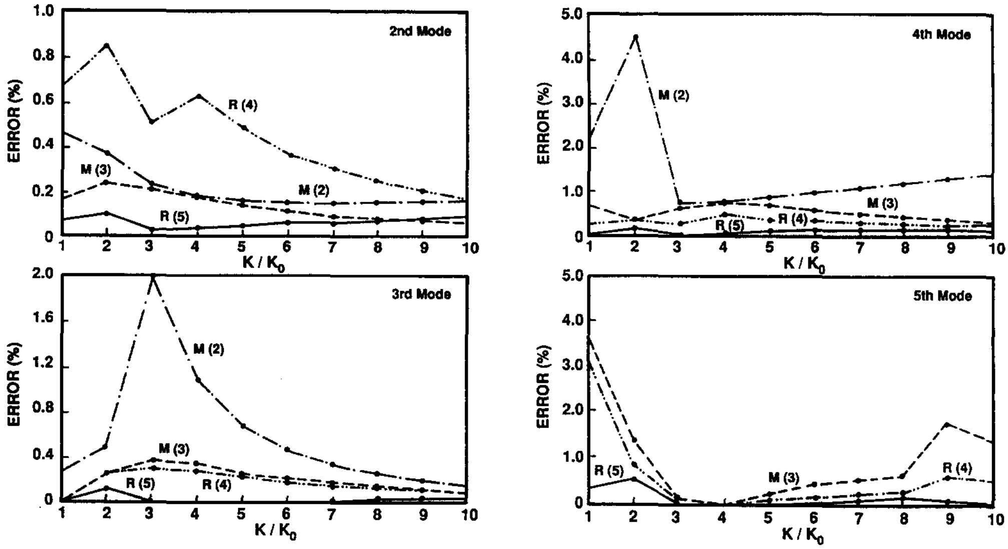

Fig. 4. The relative errors in the natural frequencies of the uniform beam (using free-substructure method).

(c) Case 3—$M(2)$, in which two natural modes for each substructure are employed in the analysis; and

(d) Case 4—$M(3)$, in which three natural modes for each substructure are employed in the analysis.

The total generalized coordinates of the full beam are the sum of the number of Ritz vectors (or modes) for all the substructures. The relative errors associated with the first natural frequency are nearly equal to zero for all cases. The relative errors in estimating the second, third, fourth, and fifth natural frequencies of the beam are shown in Fig. 4. The figure shows that the errors for the second, third, fourth and fifth mode frequencies are small and within the practical acceptable limits. There appears to be a tendency for the error to peak around K/K_0 equal to 3 in some cases and a value equal to 2 or 4 in others. In general, the frequency error is low for a very high (or a very low) K/K_0 value. As a result, a local error peak is to be expected in some of the cases.

(iii) *Effect of the symmetry of the substructure.* To illustrate the significance of the symmetrical function, $\{\mathbf{S}_i\}$, in determining the weighted function vector, $\{\mathbf{w}_i\}$, symmetrical and asymmetrical forms of $\{\mathbf{w}_i\}$ are assumed in determining the three Ritz vectors associated with each fixed-interface substructure. Then, the six Ritz vectors and the two constraint modes are employed in synthesizing the natural frequencies of the full beam. The resulting relative errors in estimating the natural frequencies are listed in Tables 1 and 2, for both forms of $\{\mathbf{w}_i\}$, respectively. Apart from the first two frequencies for the symmetrical form of $\{\mathbf{w}_i\}$, the results are clearly poor.

Table 1. Percentage relative errors of the natural frequencies of the beam (using symmetrical $\{\mathbf{f}_i(\mathbf{s})\}$)

	K/K_0									
f_i	1	2	3	4	5	6	7	8	9	10
f_1	0.12	0.12	0.12	0.12	0.12	0.12	0.12	0.12	0.12	0.12
f_2	0.16	0.06	0.03	0.02	0.01	0.01	0.01	0.00	0.00	0.00
f_3	9.54	18.10	29.41	42.36	42.36	42.36	42.36	42.36	42.36	42.36
f_4	42.36	42.36	39.73	35.63	43.56	50.64	56.83	62.15	66.66	70.46
f_5	69.19	61.13	54.37	48.96	45.12	40.60	40.60	36.99	34.13	33.78

Table 2. Percentage relative errors of the natural frequencies of the beam (using asymmetrical $\{\mathbf{f}_i(\mathbf{s})\}$)

	K/K_0									
f_i	1	2	3	4	5	6	7	8	9	10
f_1	32.08	32.08	32.08	32.08	32.08	32.08	32.08	32.08	32.08	32.08
f_2	41.84	76.67	102.60	121.40	131.70	143.20	150.30	154.90	158.20	160.70
f_3	65.14	40.71	31.74	31.74	31.74	31.74	31.74	31.74	31.74	31.74
f_4	38.28	41.64	43.35	41.74	43.47	47.06	51.69	56.86	62.28	67.78
f_5	151.60	137.70	125.10	114.60	106.30	99.70	94.60	90.53	90.03	90.03

(2) *Example* 2

In this example, a beam that differs from the one used in Example 1 in the values assumed for its stiffness, EI, is employed. Five EI values are assumed such that $(EI)_1 = 40{,}600$ kN cm^2 (for elements 1, 4, 7, 8, 10, 12, 15 and 16); $(EI)_2 = 72{,}384$ kN cm^2 (for elements 2 and 13); $(EI)_3 = 75{,}863$ kN cm^2 (for elements 3 and 9); $(EI)_4 = 68{,}904$ kN cm^2 (for elements 5 and 11); and $(EI)_5 = 63{,}220$ kN cm^2 (for elements 6 and 14). If the fixed-interface CMS method is applied to this beam, obviously, the stiffness matrices of the fixed-interface substructures would have no symmetry; however, their mass matrices would still have symmetry. Four computational cases: $R(3)$, $R(4)$, $M(2)$ and $M(3)$, are considered. The relative errors for the third, fourth and fifth natural frequencies of the full beam in these cases are shown in Fig. 5. In both cases of $R(3)$ and $R(4)$, the symmetry function, $\{\mathbf{S}_i\}$, is accounted for in determining the weighted function vector, $\{\mathbf{w}_i\}$, for both substructures. For comparison purposes, the case of $R(3)$ is considered again using $\{\mathbf{w}_i\}$ in which the symmetry function, $\{\mathbf{S}_i\}$, is not included, i.e. all elements of $\{\mathbf{S}_i\}$ are equal to

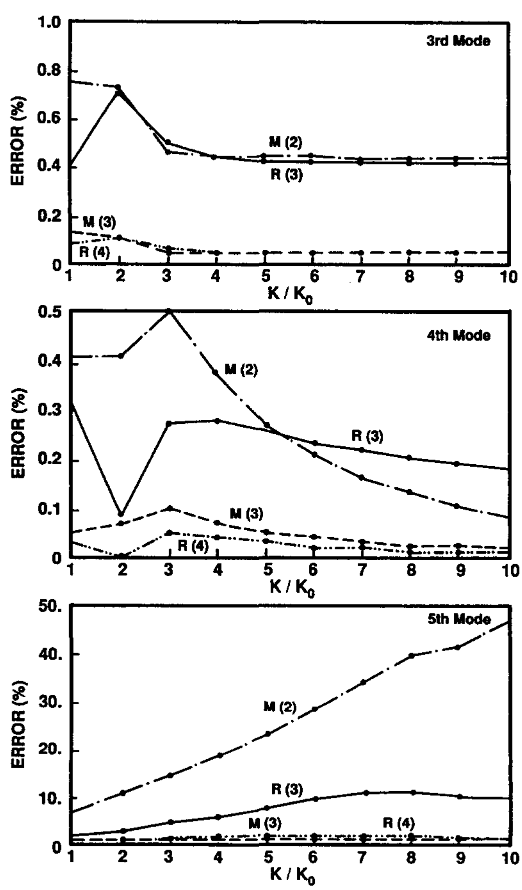

Fig. 5. The relative errors in the natural frequencies of the non-uniform beam (using fixed-substructure method).

Table 3. Percentage relative errors of the natural frequencies of the beam (using symmetrical $\{\mathbf{f}_i(\mathbf{s})\}$)

	K/K_0									
f_i	1	2	3	4	5	6	7	8	9	10
f_3	2.93	5.27	7.54	7.54	7.84	7.93	7.87	7.99	8.01	8.03
f_4	8.39	8.78	8.90	8.90	10.48	11.81	12.82	13.59	14.19	15.05
f_5	18.08	15.74	13.75	13.75	12.35	11.59	11.43	11.77	12.33	13.41

unity and $\{\mathbf{w}_i\}$ is symmetrical. The corresponding results are given in Table 3. Employing the same number of Ritz vectors (i.e. 3), the results, for this case, are clearly much worse than the corresponding results shown in Fig. 5.

7. CONCLUSIONS

A new definition for the spatial distribution vector has been proposed for the application of Wilson–Ritz vectors in CMS methods. Based on the work presented in this paper, the following can be concluded:

(1) A recurrence algorithm as given by eqns (8a, b) and (9a, b) for determining the elastic restoring force, [**P**], and the reduced stiffness matrix, [**K***], of the substructure in the subspace spanned by the obtained Ritz vectors, is attainable in the coordinate transformation systems of the substructures.

(2) It is essential to introduce the symmetry function into the weighted function vector for symmetrical (or partially symmetrical) substructures when the Ritz CMS is applied to modal analysis of the structure. Significant errors can result if this was not performed as demonstrated by examples.

(3) Excellent results can be achieved using Ritz CMS methods. Moreover, the computational effort can be also reduced. In general, more Ritz vectors than the normal modes of a substructure are required in order to achieve the same accuracy. In the examples discussed in this paper, it was observed that one (or two) more Ritz vectors are required for each substructure. In the meantime, a saving of computational effort is achieved.

Acknowledgements—The work done in this study has been supported by the National Natural Science Foundation of China and the Natural Sciences and Engineering Research Council (NSERC) of Canada. The authors are grateful for this support.

REFERENCES

Abdallah, A. A. and Huckelbridge, A. A. (1990). Boundary flexible method of component mode synthesis using static Ritz vectors. *Comput. Struct.* **35**, 51–61.

Arnold, R. R. Citerley, R. L., Chargin, M. and Galant, D. (1985). Application of Ritz vectors for dynamic analysis of large structures. *Comput. Struct.* **21**, 461–467.

Benfield, W. A. and Hruda, R. F. (1971). Vibration analysis of structures by component mode substitution. *AIAA Jl* **9**, 1255–1261.

Craig, R. R., Jr and Bampton, M. C. C. (1968). Coupling of substructures for dynamic analysis. *AIAA Jl* **6**, 1313–1319.

Hurty, W. C. (1965). Dynamic analysis of structural systems using components modes. *AIAA Jl* **3**, 678–685.

Lou, M. and Lian, W. (1989). Synthesis method of Ritz vectors of substructures without coupling interface. *J. Vibr. Shock* **8**(2), 40–44 (in Chinese).

MacNeal, R. H. (1971). A hybrid method of component mode synthesis. *Comput. Struct.* **1**, 581–601.

Rubin, R. (1975). Improved component-mode representation for structural dynamic analysis. *AIAA Jl* **13**, 995–1006.

Wang, W. and Du, Z. (1985). *Structure Vibration and Dynamic Substructure Methods* (in Chinese). Press of Fudan University, China.

Wilson, E. L. and Bay, E. P. (1986). Use of spatial Ritz vectors in dynamic substructure analysis. *J. Struct. Engng Div., ASCE* **112**, 1944–1954.

Wilson, E. L., Yuan, M.-W. and Dickens, J. M. (1982). Dynamic analysis by direct superposition of Ritz vectors. *Earthquake Engng Struct. Dynam.* **10**, 813–823.